Improving the hydrology of the Simple Biosphere Model 2 and its evaluation within the framework of a distributed hydrological model

LEI WANG[1], TOSHIO KOIKE[1], DAWEN YANG[2] & KUN YANG[3]

1 *Department of Civil Engineering, The University of Tokyo, Hongo 7-3-1, Bunkyo-ku, Tokyo 113-8656, Japan*
wang@hydra.t.u-tokyo.ac.jp

2 *Department of Hydraulic Engineering, Tsinghua University, Beijing 100084, China*

3 *Institute of Tibetan Plateau Research, Chinese Academy of Sciences, Beijing 100085, China*

Abstract The hydrological description of the Simple Biosphere Model 2 (SiB2) is improved in three respects. First, the SiB2 three-layer soil model is replaced with a multi-layer soil column coupled to a lumped unconfined aquifer model. Next, lateral water flows are described in the updated soil model. Finally, the soil hydraulic function in SiB2 is replaced with van Genuchten parameterization, and exponential vertical soil heterogeneity is described. In using observed streamflow to evaluate the hydrologically improved SiB2 (HydroSiB2), a new hydrological model (HydroSiB2-DHM) was developed by embedding HydroSiB2 into the spatial framework of a distributed hydrological model. Three-year fine temporal scale meteorological data from a small river basin were used to drive both HydroSiB2-DHM and SiB2-DHM (the same as HydroSiB2-DHM but with the original SiB2). Sub-grid topography was considered in both model runs, and analyses were based on basin-averaged values to maintain consistency with the regional evaluation using streamflow. The results show that HydroSiB2-DHM performs well in both fine and coarse time-scale runoff simulations; while SiB2-DHM captures inter-annual and seasonal runoff changes, but gives poor results in simulations at finer temporal-scales (daily and hourly). Owing to the treatment of lateral flows and using a multi-layer soil model coupled with a lumped unconfined aquifer in HydroSiB2, the soil moisture budget is qualitatively improved. In recession periods, the basin-averaged bare soil evaporation reduced by about 0.1 mm/d, resulting in a decrease in the latent heat flux and an increase in sensible heat flux of about 3.9 and 3.2 W/m^2, respectively.

Key words SiB2; HydroSiB2; distributed hydrological model; streamflow; soil wetness; evapotranspiration; sensible heat flux; lateral flows

Amélioration de l'hydrologie du Modèle Simple de Biosphère 2 et son évaluation dans le cadre d'un modèle hydrologique distribué

Résumé La description hydrologique du Modèle Simple de Biosphère (SiB2) est améliorée à trois égards. D'abord, le modèle de sol à trois couches de SiB2 est remplacé par une colonne de sol multi-couches couplée à un modèle global d'aquifère libre. Puis les écoulements latéraux sont décrits dans le modèle de sol mis à jour. Enfin la fonction hydraulique du sol dans SiB2 est remplacée par la paramétrisation de van Genuchten, et l'hétérogénéité verticale exponentielle du sol est décrite. La version améliorée sur le plan hydrologique de SiB2 (HydroSiB2) étant évaluée compte tenu de l'écoulement observé en cours d'eau, un nouveau modèle hydrologique (HydroSiB2-DHM) a été développé en inscrivant HydroSiB2 dans le cadre spatial d'un modèle hydrologique distribué. Trois ans de données météorologiques fines d'un petit bassin versant ont été utilisées pour piloter HydroSiB2-DHM et SiB2-DHM (similaire à HydroSiB2-DHM mais avec le SiB2 original). La topographie infra-maille a été considérée dans les deux mises en œuvre de simulation, et les analyses ont été basées sur des valeurs moyennes pour le bassin versant afin de conserver la cohérence avec l'évaluation régionale basée sur l'écoulement en cours d'eau. Les résultats montrent que HydroSiB2-DHM a de bonnes performances pour la simulation de l'écoulement aux échelles de temps fines et larges; tandis que SiB2-DHM capture les changements interannuels et saisonniers d'écoulement, mais donne de pauvres résultats de simulation aux échelles de temps plus fines (quotidiennes et horaires). En raison du traitement des écoulements latéraux et de l'utilisation d'un modèle de sol multi-couches couplé à un modèle global d'aquifère libre dans HydroSiB2, le bilan de l'humidité du sol est qualitativement amélioré. En périodes de récession, l'évaporation sur sol nu moyenne pour le bassin versant est réduite d'environ 0.1 mm/jour, ce qui induit une diminution du flux de chaleur latente et une augmentation du flux de chaleur sensible d'environ 3.9 et 3.2 W/m^2 respectivement.

Mots clefs SiB2; HydroSiB2; modèle hydrologique distribué; écoulement en cours d'eau; humidité du sol; évapotranspiration; flux de chaleur sensible; écoulements latéraux

INTRODUCTION

Over the last several decades, land surface models (LSMs) have evolved from simple bucket models without vegetation consideration (e.g. Manabe, 1969) into credible representations of the

exchanges of energy, water and carbon dioxide in soil–vegetation–atmosphere transfer (SVAT) systems (e.g. Sellers *et al*., 1996a; Dickinson *et al*., 1998). Despite the increasing complexity of LSMs, the hydrology in most of them needs to be further improved.

The Project for the Intercomparison of Land-surface Parameterization Schemes (PILPS) aims at improving the understanding of LSMs in climate and weather forecast modelling (Henderson-Sellers *et al*., 1993). Runoff parameterizations were compared among all the LSMs participating in PILPS. It was found that most LSMs tend to treat runoff as the excess of water in the soil reservoir, without considering the sub-grid-scale distribution of topography and lateral water flow processes. Some earlier SVAT systems only include overland flow (e.g. Manabe, 1969), while more advanced ones also incorporate gravitational drainage (e.g. Sellers *et al*., 1986). However, owing to the omission of modelling topographically driven lateral flows from vertical soil columns in LSMs, the surface soil layer likely remains wet too long after a rainfall event (Soulis *et al*., 2000). Consequently, latent heat flux (evapotranspiration) will be overestimated between rainfall events, corrupting the calculation of atmospheric fluxes.

Recently, the importance of modelling groundwater dynamics in LSMs has been recognized (e.g. Yeh & Eltahir, 2005; Gulden *et al*., 2007; Maxwell *et al*., 2007; Niu *et al*., 2007); groundwater interacts with soil moisture through the exchange of water between the groundwater aquifer and its overlying unsaturated soil driven by gravity and capillary forces. However, most LSMs lack representations of the groundwater–surface water interactions, which could result in large errors in the simulation of water and energy fluxes of the land surface, especially for the shallow water table areas in humid regions (Yeh & Eltahir, 2005). Gulden *et al*. (2007) used Monte Carlo analysis to show that explicit representation of a groundwater aquifer within a LSM decreases the dependence of the model performance on accurate selection of subsurface hydrological parameters. Therefore, groundwater table dynamics should be represented in LSMs because the groundwater–atmosphere interaction has a potentially significant influence on spatial and temporal climate variability.

On the other hand, soil can store and transport water, and thus affect the behaviour of the vegetation cover and the turbulent fluxes determining the development of the atmosphere. Soil hydraulic conductivity determines the amount of water transporting in soils, which directly changes the soil moisture distribution in both vertical and lateral directions. Many studies showed that accurately estimating soil moisture and its spatial distribution is critical for atmospheric model forecasts (e.g. Pielke, 2001; Findell & Eltahir, 2003). Braun & Schadler (2005) compared seven soil hydraulic parameterizations used in mesoscale meteorological models, including the Campbell/Clapp-Hornberger parameterization (Campbell, 1974; Clapp & Hornberger, 1978) that is often used by meteorologists, and the van Genuchten/Rawls-Brakensiek parameterization (van Genuchten, 1980; Rawls & Brakensiek, 1982) that is used widely among hydrologists. In their numerical experiments, the performance achieved using the van Genuchten/Rawls-Brakensiek model was better than that achieved using the Campbell/Clapp-Hornberger model in simulating soil water contents. Therefore, it is also critical to deal with soil hydraulic functions in LSMs for better estimation of the soil moisture distribution.

The improvements in LSM hydrology have drawn much attention among the atmospheric scientific community (e.g. Lohmann *et al*., 1998; Boone *et al*., 2004; Yeh & Eltahir, 2005; Decharme & Douville, 2006; Decharme *et al*., 2006; Gulden *et al*., 2007; Niu *et al*., 2007). However, up to now, little attention has been paid to improving the hydrology of the biosphere scheme SiB2, except for the work by Tang *et al*. (2006, 2008), even though SiB2 has been used extensively for surface flux estimations in numerical models (e.g. Randall *et al*., 1996; Entin *et al*., 1999; Gao *et al*., 2004; Bounoua *et al*., 2006).

The simple biosphere model (SiB) (Sellers *et al*., 1986) is a simple, but realistic, biosphere model developed for calculating the transfer of energy, mass and momentum between the atmosphere, land surface and soil. Its revised version (SiB2) has incorporated several improvements, including a canopy photosynthesis–conductance sub-model, as well as the use of satellite data to describe the vegetation state and phenology (Sellers *et al*., 1996a). Compared to its

first version (SiB), SiB2 can give a better description of baseflow and a more reliable calculation of interlayer exchanges within the soil profile, with basic treatment of the reduction of conductivity and baseflow when the temperature drops below freezing. However, like many LSMs, SiB2 only includes elementary runoff components of infiltration excess (Horton runoff; Freeze, 1974) and gravitational outflow, without a treatment of lateral water redistributions due to uneven sub-grid topography, a representation of groundwater table dynamics, or a description of vertical soil heterogeneity.

The approach of this paper is to improve the hydrology of SiB2 by benefiting from a previous distributed hydrological model—the geomorphology-based hydrological model (GBHM) (Yang *et al*., 2000, 2002, 2004; Wang *et al*., 2006). In this study, several significant improvements have been made to enhance the hydrology in SiB2. Firstly, the SiB2 three-layer soil model is replaced by a multi-layer soil column coupled to a lumped unconfined aquifer model, which simultaneously receives the recharge from the upper soils and discharges runoff into rivers. The total thickness of the unsaturated soil changes with the fluctuations of the water table. Secondly, lateral water flows are described in the updated soil model. Overland flow is described by Manning's equation, while lateral subsurface flow and groundwater discharge are simulated using Darcy's law. Thirdly, the soil hydraulic function in SiB2 (the Campbell/Clapp-Hornberger parameterization) is updated with the van Genuchten function, and soil vertical heterogeneity is described. The hydrologically improved SiB2 (hereafter referred to as HydroSiB2) is then embedded into the distributed framework of the GBHM to develop a new model (hereafter referred to as HydroSiB2-DHM), by which the improved SiB2 hydrology can be evaluated by comparing simulated and observed discharges at stream gauges in a watershed.

IMPROVEMENTS OVER SIB2 HYDROLOGY

Soil model

As shown in Fig. 1(a), SiB2 uses a three-layer soil model comprising a surface layer (D_1), root zone (D_2) and deep soil zone (D_3). The uppermost thin soil layer acts as a significant source of direct evaporation when moist. The roots are assumed to access the soil moisture from the second

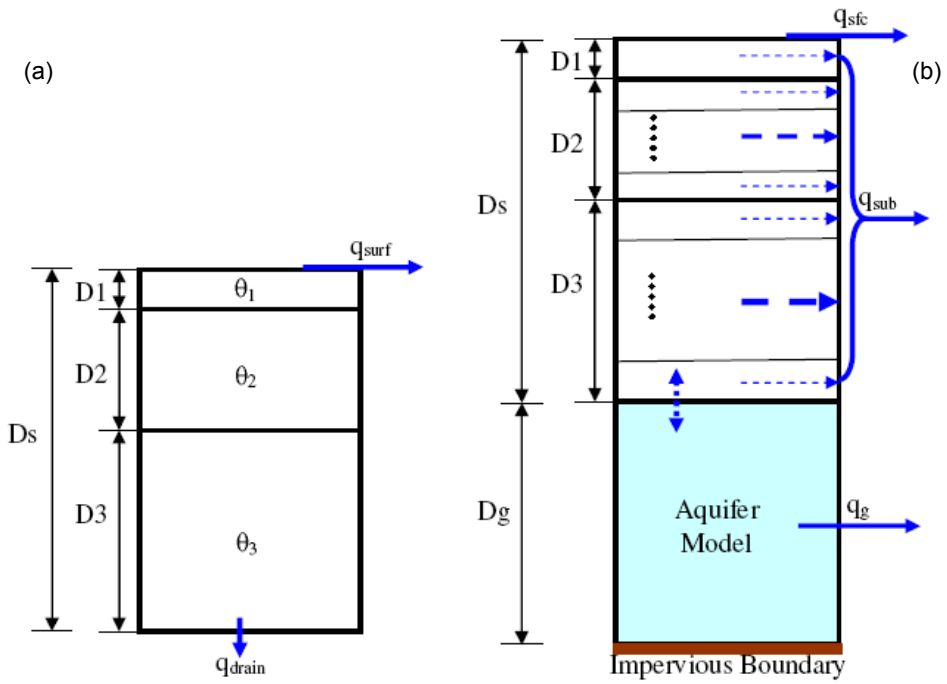

Fig. 1 Soil models used: (a) in SiB2, and (b) in HydroSiB2.

layer (root zone), while the third layer (deep soil zone) acts as a source for hydrological baseflow and upward recharge of the root zone. Water table dynamics are not described in SiB2.

In HydroSiB2, the old soil model in SiB2 is replaced by a multi-layer soil column coupled to a lumped unconfined aquifer model with an impermeable lower boundary (see Fig. 1(b)). The groundwater aquifer simultaneously receives the recharge from the upper soils and discharges runoff into rivers. The total thickness of the unsaturated soil changes with fluctuations of the water table. For more accurate estimation of soil moisture, the root zone and deep soil zone are sub-divided into several sub-layers. The vertical inter-layer flows in the unsaturated zone are described using a one-dimensional Richards equation. The continuity equation of vertical moisture movement in the unsaturated zone can be written as:

$$\frac{\partial \theta(z,t)}{\partial t} = -\frac{\partial q_v}{\partial z} + s(z,t) \tag{1}$$

where t is time, z is the distance from the surface measured vertically downward (m), $\theta(z, t)$ is the volumetric water content, $s(z, t)$ is the source or sink of evaporation and transpiration. q_v represents the soil moisture flux in the vertical direction and is given as:

$$q_v = -K(\theta, z)\left[\frac{\partial \psi(\theta)}{\partial z} - 1\right] \tag{2}$$

where $K(\theta, z)$ is hydraulic conductivity and $\psi(\theta)$ is capillary suction (m).

Lateral water flows

The lateral flows are described in the updated soil model. Overland flow is described by Manning's equation, while lateral subsurface flow and groundwater discharge are simulated using Darcy's law.

Lateral subsurface flow After the calculation of water moisture exchanges between sub-layers of the unsaturated zone in the vertical direction, the lateral subsurface flow is simulated. For all unsaturated sub-layers above the water table, when soil moisture content (θ) is greater than the field capacity (θ_f), the soil water of the sub-layer moves due to gravity towards the stream. The lateral subsurface flow of each sub-layer (q_{sub}) is described by:

$$q_{\text{sub}} = \begin{cases} K(\theta)\sin X & \theta > \theta_f \\ 0 & \theta \le \theta_f \end{cases} \tag{3}$$

where $K(\theta)$ is the hydraulic conductivity in a sub-layer and X is the grid slope. The continuity equation of lateral moisture movement in the unsaturated zone can be written as:

$$\frac{q_{\text{sub}}}{\Delta z_i} = \frac{\partial \theta(z,t)}{\partial t} \tag{4}$$

where Δz_i is the thickness of the ith sub-layer.

Groundwater flow In HydroSiB2, the water table dynamics of the lumped aquifer model are described as in the work by Yang *et al*. (2000). The basic equations used for the saturated zone (unconfined aquifer) are mass balance and Darcy's law. The mass balance is described by:

$$\frac{\partial S_G}{\partial t} = \text{rech} - q_g \frac{1000}{A_h} \tag{5}$$

where S_G is the groundwater storage (S_G = GWcs(D_s + D_g – WDT); GWcs is the groundwater storage coefficient; D_s and D_g are the initial thickness for the unsaturated zone and saturated zone, respectively (shown in Fig. 1(b)); WTD is the water table depth taken downward in a direction normal to the soil surface; rech is the recharge rate from the upper unsaturated zone; and A_h is the

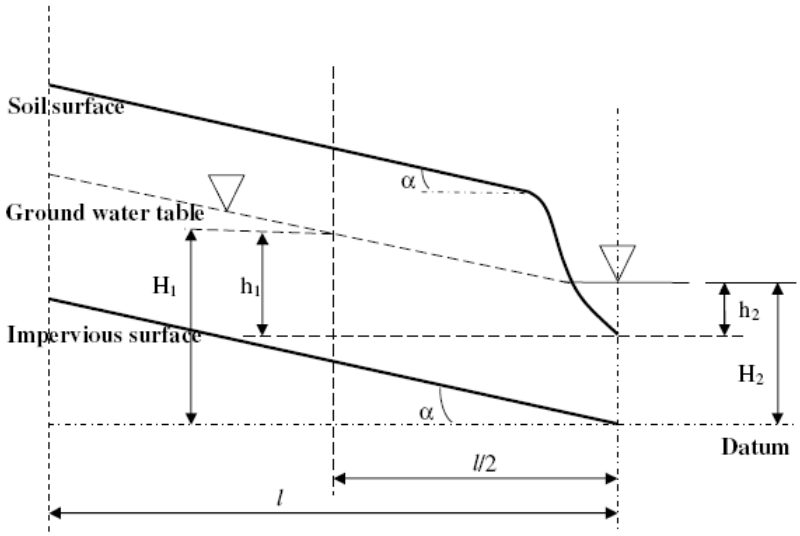

Fig. 2 Hillslope element used in GBHM (reproduced from Yang *et al*., 2002).

plane area of the hillslope element. The exchange (q_g) between the groundwater and the river is considered as steady flow and is calculated using Darcy's law:

$$q_g = K_g \frac{H_1 - H_2}{l/2} \frac{h_1 + h_2}{2} \tag{6}$$

where K_g is the hydraulic conductivity of the unconfined aquifer; l is the length of the hillslope; and H_1, H_2, h_1 and h_2 are illustrated in Fig. 2.

When the water table depth (WTD) of a grid is higher than the river water level, groundwater flows into the river and the WTD increases; otherwise, river water recharges the groundwater. After the calculation of this water exchange, the new WTD of the grid is determined.

Overland flow In SiB2, overland flow is defined as precipitation excess, which is equal to the effective precipitation on the soil surface minus the infiltration into the surface soil. In HydroSiB2, after the calculation of the vertical moisture exchanges, the overland flow is described by steady constant sheet flow using Manning's equation:

$$q_{\text{sfc}} = \frac{1}{n}(\sin X)^{1/2} h^{5/3} \tag{7}$$

where q_{sfc} is the overland flow for one hillslope unit, n is Manning's roughness parameter, X is the grid slope, and h is water depth.

The entire continuity equation including surface flow, lateral subsurface flow, groundwater flow and evapotranspiration can be described as:

$$q_{\text{sfc}} + \sum q_{\text{sub}} + q_G = \frac{\mathrm{d}P}{\mathrm{d}t} - \frac{\mathrm{d}I}{\mathrm{d}t} - \frac{\mathrm{dET}}{\mathrm{d}t} - \frac{\mathrm{d}S}{\mathrm{d}t} \tag{8}$$

where $\sum q_{\text{sub}}$ is the total lateral subsurface flows for one hillslope unit; P is precipitation; I is interception by canopy and ground; ET is evapotranspiration; S is the total water storage in the unsaturated and saturated zones.

Soil hydraulic function and vertical soil heterogeneity

Table 1 shows the soil hydraulic functions used in SiB2 and HydroSiB2. In SiB2, the Campbell/Clapp-Hornberger parameterization (Clapp & Hornberger, 1978) is adopted. However, comparisons among seven soil hydraulic parameterizations used in mesoscale meteorological

Table 1 Soil hydraulic functions used in SiB2 and HydroSiB2.

Source	$\psi(\theta)$	$K(\theta)/K_s$
Campbell (1974)	$\psi_s(\theta/\theta_s)^{-b}$	$(\theta/\theta_s)^{2b+3}$
van Genuchten (1980) *	$(1/\alpha)\,(S^{-1/m})^{1/n}$	$S^{1/2}[1-(1-S^{-1/m})^m]^2$

* $S = (\theta - \theta_r)(\theta_s - \theta_r)$; where θ_s is saturation water content and θ_r is residual water content; ψ_s is soil moisture potential at saturation; K_s is the hydraulic conductivity at saturation; b is the empirical parameter used in Campbell function, while α, n are empirical parameters in van Genuchten's equation with $m = 1 - 1/n$.

models show that the van Genuchten/Rawls-Brakensiek model performs better than the Campbell/Clapp-Hornberger model in simulating soil water contents for the cases and soil types considered by Braun & Schadler (2005). For more accurate simulation of soil water contents, HydroSiB2 takes the van Genuchten function (van Genuchten, 1980) as its soil hydraulic function, which can easily use soil parameters defined by Rawls & Brakensiek (1982) together with soil texture information.

In HydroSiB2, the non-uniform vertical distribution is represented using the assumption of an exponential decrease in hydraulic conductivity with increasing soil depth (Cabral *et al*., 1992; Robinson & Sivapalan, 1996):

$$K_s(z) = K_0 \exp(-fz) \tag{9}$$

where $K_s(z)$ is the saturated hydraulic conductivity at depth z, which is measured downward in a direction normal to the soil surface (m), K_0 is the saturated conductivity at the surface (mm/h), and f is the hydraulic conductivity decay parameter.

EVALUATION METHODOLOGY AND DATA SETS

Evaluation methodology

The hydrologically improved SiB2 (HydroSiB2) is embedded into the distributed framework of the grid-based version of the GBHM (Yang *et al*., 2004) to develop a new hydrological model (HydroSiB2-DHM), replacing the original vertical scheme in the GBHM to describe the soil–vegetation–atmosphere transfer (SVAT) system. Through this methodology, HydroSiB2 can be evaluated by comparing simulated and observed streamflow at the measuring points in a watershed. The overall model structure of HydroSiB2-DHM can be described as follows:

(a) A digital elevation model (DEM) is used to define the target area and then the target basin is divided into sub-basins. Sub-grid topography is considered if a finer DEM is available.
(b) Within a given sub-basin, a number of flow intervals are specified to represent time lag and accumulating processes in the river network according to the distance to the outlet for the sub-basin. Each flow interval includes several model grids.
(c) Each model grid is subdivided into a number of geometrically symmetrical hillslopes. For each hillslope, HydroSiB2 simulates turbulent fluxes (water, energy and CO_2) and lateral runoff comprised of overland, lateral subsurface and groundwater flows. Runoff for a model grid is the total lateral runoff from all hillslopes in it.

To simulate flow routing in a river network, the Pfafstetter scheme (Pfafstetter, 1989; Verdin & Verdin, 1999) is applied for subdividing the basin and for numbering the flow sequence among the sub-basins. A virtual channel is allocated for each flow interval. Therefore, the river network of a sub-basin is simplified such that only the main river is considered. The lateral inflow (q_{lateral}) into the main river from each flow interval is the total runoff generated from all of the model grids in the same flow interval. The flow sequences among these simplified main rivers are defined by the codes of the divided sub-basins. The flow routing of the entire river network in the basin is modelled using the kinematic wave approach. The continuity equation is:

$$\frac{\partial Q}{\partial x} + \frac{\partial A}{\partial t} = q_{\text{lateral}} \tag{10}$$

and the momentum equation is given by Manning's equation as:

$$Q = \frac{S_r^{1/2}}{np^{2/3}} \cdot A^{5/3} \tag{11}$$

where Q is the discharge at a the distance x along the longitudinal axis of the river, A is the cross-sectional area, t is time, S_r is the river bed slope, n is Manning's roughness parameter, and p is the wetted perimeter.

To demonstrate the improvements in SiB2 hydrology, the original SiB2 was also coupled with the spatial framework of the grid-based GBHM (Yang *et al*., 2004) to obtain another model (hereafter SiB2-DHM). Using available data of observed streamflow, the hydrological improvements of HydroSiB2 over SiB2 can be illustrated by comparing the results simulated by SiB2-DHM and HydroSiB2-DHM.

Data sets

Validation requires highly accurate data. Therefore, a small basin (Agatsuma, in Japan; see Fig. 3(a)) for which fine observations have been conducted was selected to compare the performances of HydroSiB2 and SiB2 by routing their runoff responses to stream gauges through a distributed hydrological framework.

The Agatsuma River basin, a sub-basin of the upper Tone River basin, is located northwest of Tokyo (Fig. 3(a)). The elevation of this basin varies from about 200 to 2500 m (Fig. 3(b)). The catchment area lying upstream of the Murakami gauge is about 1300 km^2. Only a very small reservoir was completed in the upper stream of the Agatsuma River basin and it was not considered in this study. Heavy rainfall events commonly occur from June to October (flood season) and are associated with typhoons and Mei-yu front activity.

The DEM and land-use data were obtained from the Japan Geographical Survey Institute. Sub-grid topography was described by a 50-m resolution DEM. Land-use data were reclassified into three SiB2 categories, with broadleaf-deciduous trees being the dominant land use type (more than 85%; Fig. 3(b)). The static vegetation parameters comprising morphological properties, optical properties and physiological properties were defined following Sellers *et al*. (1996b). The dynamic vegetation parameters were leaf area index (LAI) and the fraction of photosynthetically active radiation absorbed by the green vegetation canopy (FPAR), which can be obtained from satellite data. Global LAI and FPAR MOD15_BU 1-km data sets (Myneni *et al*., 1997) were used in this study, which are 8-daily composites of MOD15A2 products and were provided by the Earth Observing System Data Gateway of the National Aeronautics and Space Administration.

Soil type was determined from a 1:200 000 scale Gunma Prefecture geological map (Fig. 3(b)). In this paper, we set related soil static parameters (see Table 2) following a previous study in the upper Tone River basin by Yang *et al*. (2004). According to the empirical parameters (α and n) defined in the van Genuchten equation, the parameter b used in the Campbell function was calibrated to minimize the difference in the relative hydraulic conductivities used in SiB2-DHM and HydroSiB2-DHM (see Fig. 4). Owing to lack of geological data, the initial thickness of the unsaturated zone (D_s) was defined as 4 m following the Food and Agriculture Organization global soil type map (FAO, 2003).

Hourly precipitation data were obtained from the radar-Automated Meteorological Data Acquisition System (AMeDAS) rainfall analysis data, which are a combination of both radar and ground observations, provided by the Japanese Meteorological Agency (JMA). The data are available at 5-km spatial resolution for before March of 2001 and at 2.5-km spatial resolution for later times. The surface meteorological parameters other than precipitation are air temperature, relative humidity, air pressure, wind speed, and downward solar and long-wave radiation. Air temperature, wind speed, and sunshine duration were taken from the AMeDAS annual report of the JMA. In our study basin, the observed air temperature, wind speed, and sunshine duration data were available from three meteorological sites with hourly resolution. The downward solar

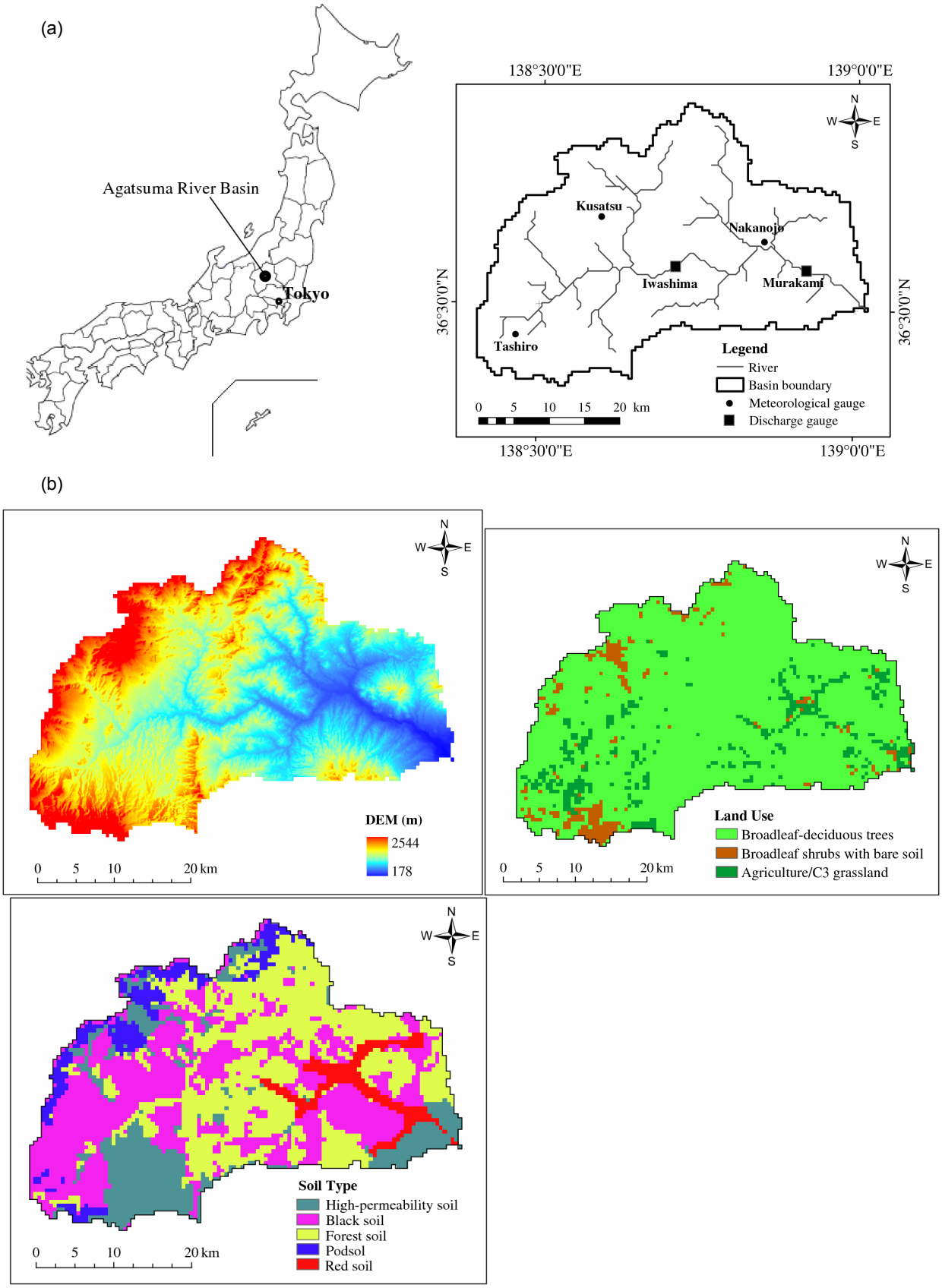

Fig. 3 (a) Location of the Agatsuma River basin, and (b) the spatial distribution of DEM, land use, and soil type.

Table 2 Soil parameters used in SiB2-DHM and HydroSiB2-DHM.

Soil type	High-permeability soil	Black soil	Forest soil	Podsol	Red soil
Coverage (%)	16	36	35	7	5
Groundwater storage coefficient (GWcs)	0.15				
Hydraulic conductivity of groundwater, K_g (mm/h)	1.0				
Saturated hydraulic conductivity for soil surface, K_s (mm/h)	80	25	50	60	60
Saturated volumetric moisture content of unsaturated zone, θ_s	0.51				
Residual volumetric moisture content of unsaturated zone, θ_r	0.17				
Parameter for soil retention curve and hydraulic conductivity in the Van Genuchten equation (1980)	$\alpha = 0.017$; $n = 1.413$				
Parameter for soil retention curve and hydraulic conductivity in the Campbell function (1974)	$b = 9.5$				

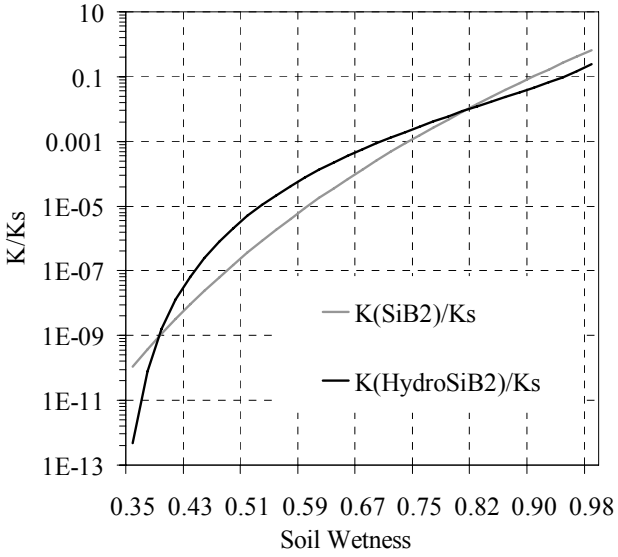

Fig. 4 Relative hydraulic conductivity (K/K_s) for SiB2 and HydroSiB2 (derived using n and b, the soil parameters used in the van Genuchten function and the Campbell function, respectively; see Table 1). The soil wetness is the ratio of the soil volumetric water content by the saturated soil volumetric water content.

radiation was estimated from sunshine duration, temperature, and humidity, using a hybrid model developed by Yang *et al*. (2001, 2006). The long-wave radiation was then estimated from temperature, relative humidity, pressure, and solar radiation using the relationship between solar radiation and long-wave radiation (Crawford & Duchon, 1999). All the inputs were interpolated to a 500-m grid for model simulations.

RESULTS AND DISCUSSION

In this study, three-year (2001–2003) meteorological data were used, and the results from the last loop of a multi-loop equilibrium simulation were analysed. Both SiB2-DHM and HydroSiB2-DHM were run with the initial soil wetness (the ratio of soil moisture to saturation soil moisture) being set at 75%. To obtain a better hydrograph, one additional equilibrium run was also performed for SiB2-DHM with a thinner D_s equal to 2 m. The results of the three equilibrium runs

were analysed. It should be mentioned that, in the study, sub-grid topography was considered in both SiB2-DHM and HydroSiB2-DHM runs. All analyses were based on basin-averaged values at the upper area of Murakami gauge to maintain consistency with the regional evaluation using observed streamflow.

Evaluation criteria

Both the Nash & Sutcliffe (1970) model efficiency coefficient (denoted as Nash) and bias error (BIAS) were used to evaluate the model performance. Nash is defined as:

$$\text{Nash} = 1 - \sum_{i=1}^{n}(Q_{\text{oi}} - Q_{\text{si}})^2 \Big/ \sum_{i=1}^{n}(Q_{\text{oi}} - \overline{Q_{\text{o}}})^2 \tag{12}$$

where Q_{oi} is the observed discharge, Q_{si} is the simulated discharge, n is the total number of time series for comparison, and $\overline{Q_{\text{o}}}$ is the mean value of the observed discharge over the simulation period. A perfect fit should have a Nash value equal to one. BIAS is defined as:

$$\text{BIAS} = \sum_{i=1}^{n}(Q_{\text{si}} - Q_{\text{oi}}) \Big/ \sum_{i=1}^{n} Q_{\text{oi}} \tag{13}$$

Analysis of results

The streamflow values for different temporal frequencies were included in analyses. Table 3 shows the annual water budgets from 2001 to 2003 simulated by SiB2-DHM and HydroSiB2-DHM. HydroSiB2-DHM represented the inter-annual variation much better than SiB2-DHM did with smaller BIAS in simulated runoff for each year, although the three-year total runoff was well estimated by both models.

Figure 5 presents the mean monthly streamflow values at Murakami gauge from 2001 to 2003. The HydroSiB2-DHM performed better in reproducing the seasonal change in runoff, with Nash equal to 0.895, than SiB2-DHM did (Nash = 0.814). Both models predicted largest runoffs in August, which was a month earlier than what was observed, but the predicted runoffs were consistent with precipitation amounts. The monthly discharge from March to June simulated by HydroSiB2-DHM is smaller than the results from SiB2-DHM; while the monthly discharge from July to September simulated by HydroSiB2-DHM is larger than SiB2-DHM. This is because, from March to June, with relatively low rainfall, SiB2-DHM simulated more baseflow ($q_{\text{drain}} = K_{\text{deep}}(\theta)\sin X$; $K_{\text{deep}}(\theta)$ is the hydraulic conductivity in D_3) than HydroSiB2-DHM, and thus saved less soil moisture in the deep soil zone. From July to September, which has a lot of rainfall, HydroSiB2-DHM generated a lot of lateral subsurface runoff due to the accumulated high soil moisture in the unsaturated zone; however, SiB2-DHM did not include the lateral subsurface runoff component. According to these reasons, HydroSiB2-DHM also showed better performances than SiB2-DHM in the daily and hourly results.

Table 3 Comparison of annual water budget for 2001–2003 simulated by SiB2-DHM and HydroSiB2-DHM.

Model	Year	P (mm)	ET (mm)	Runoff: R_{sim} (mm)	R_{obs} (mm)	BIAS (%)	ΔS (mm)
SiB2-DHM	2001	1285	580	699	818	–15	–6
	2002	1083	589	537	408	32	43
	2003	962	508	420	404	4	–34
	Mean	1110	559	552	543	7	1
HydroSiB2-DHM	2001	1285	575	790	818	–3	79
	2002	1083	583	494	408	21	–7
	2003	962	506	392	404	–3	–64
	Mean	1110	555	559	543	5	3

P: precipitation; ET: evapotranspiration; ΔS: water storage change.

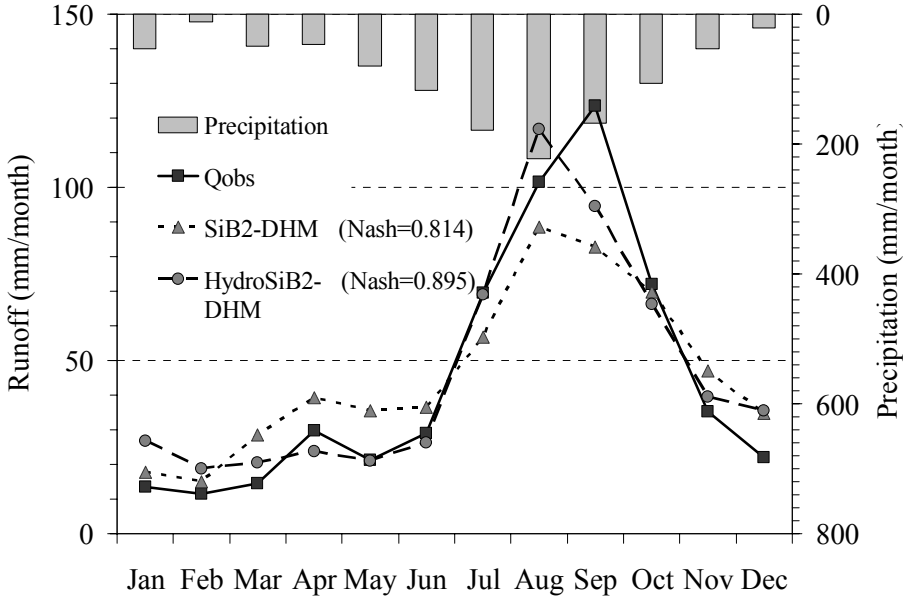

Fig. 5 Mean monthly streamflow at Murakami gauge from 2001 to 2003, simulated by SiB2-DHM and HydroSiB2-DHM.

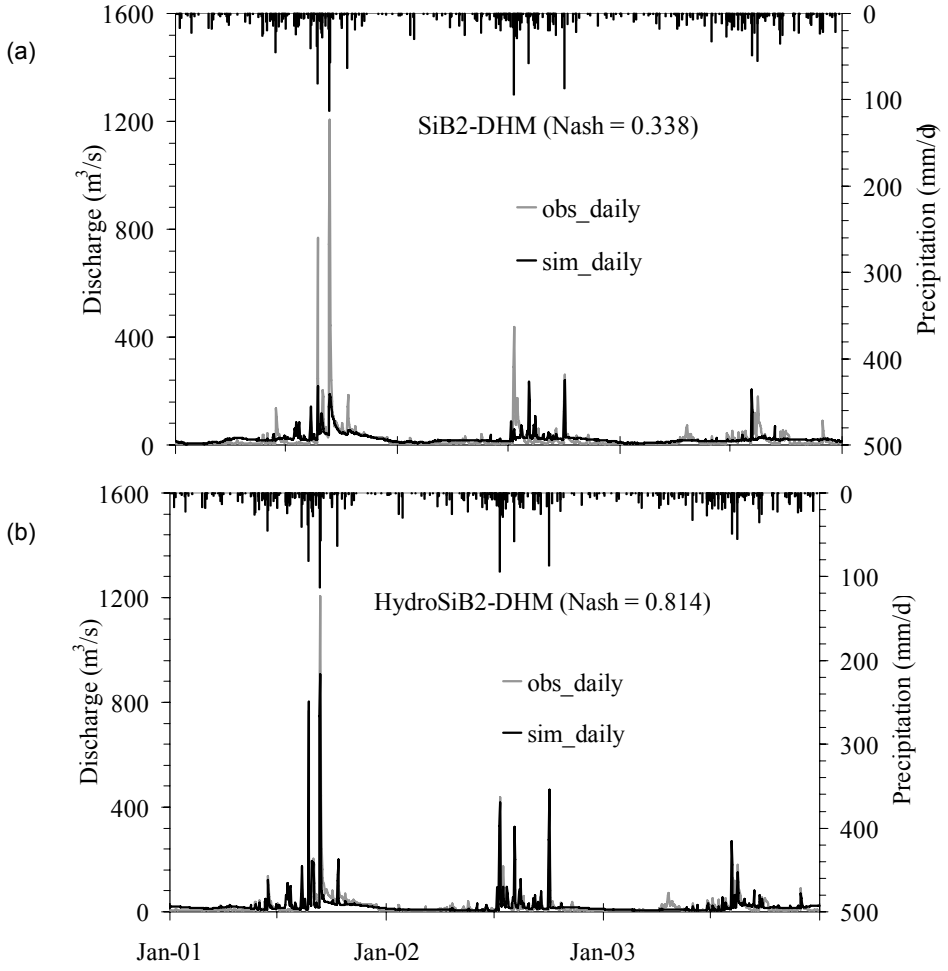

Fig. 6 Daily hydrographs at Murakami gauge from 2001 to 2003 simulated by: (a) SiB2-DHM; and (b) HydroSiB2-DHM.

Figure 6 compares the three-year (2001–2003) daily hydrographs at Murakami gauge simulated by SiB2-DHM and HydroSiB2-DHM. HydroSiB2-DHM had a reasonable response to heavy rainfall events due to the description of lateral subsurface runoff, while SiB2-DHM did not. SiB2-DHM underestimated the streamflow from July to September, but overestimated the streamflow from March to June. As a result, Nash for HydroSiB2-DHM was much higher (0.814) than that for SiB2-DHM (0.338).

Figure 7 compares the performances of the two models in simulating hourly streamflow. The hourly hydrographs show that HydroSiB2-DHM represented the fine temporal-scale hydrological processes well (Nash = 0.737), while SiB2-DHM performed even worse than it did for coarser time scales, with significant underestimation of flood peaks. The scatterplots confirm the better performance of HydroSiB2-DHM because it only slightly underestimated the hourly discharge values, while SiB2-DHM produced much lower hourly discharge than that observed, especially when the observed discharge values were greater than 100 m^3/s.

Figure 8 plots the soil wetness in the surface layer (W_{sfc}), root zone (W_{rt}), and deep soil (W_{dp}) simulated by SiB2-DHM and HydroSiB2-DHM. Without descriptions of lateral flows in SiB2, the SiB2-DHM generally gave higher surface wetness (W_{sfc}), especially in recession periods. This resulted in SiB2-DHM simulating greater bare-soil evaporation, which corrupts the calculation of latent and sensible heat fluxes. The greater deep soil wetness obtained by HydroSiB2-DHM is attributed to the incorporation of the groundwater aquifer with an impermeable lower boundary into HydroSiB2, which results in the overlying soil being wetter than that for a model without coupling to such a groundwater reservoir. The root zone wetness simulated by HydroSiB2-DHM

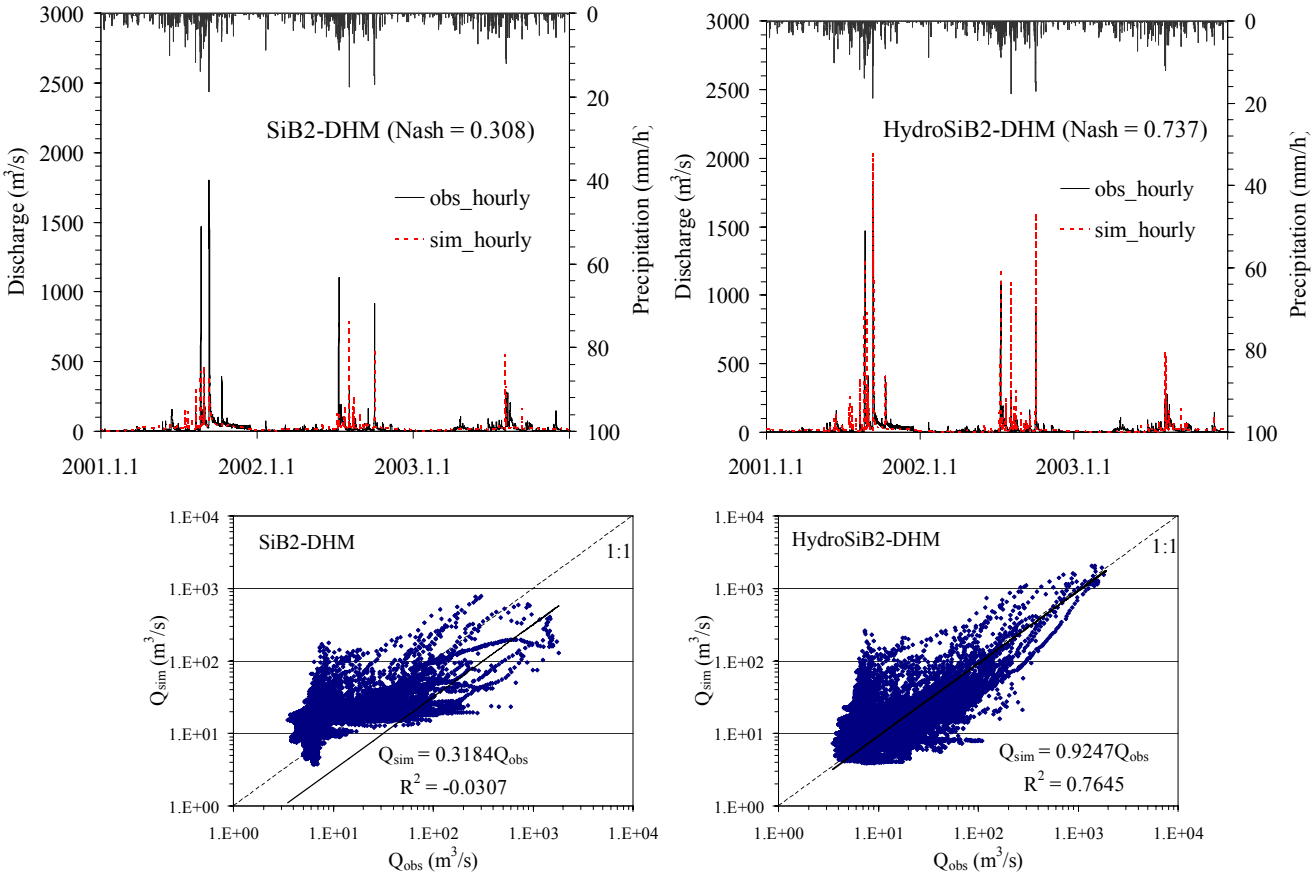

Fig. 7 Hydrographs (upper) and scatterplots (lower) of hourly discharges simulated by SiB2-DHM and HydroSiB2-DHM from 2001 to 2003. In each of the lower plots, the best fit line and a 1:1 line are included for comparison.

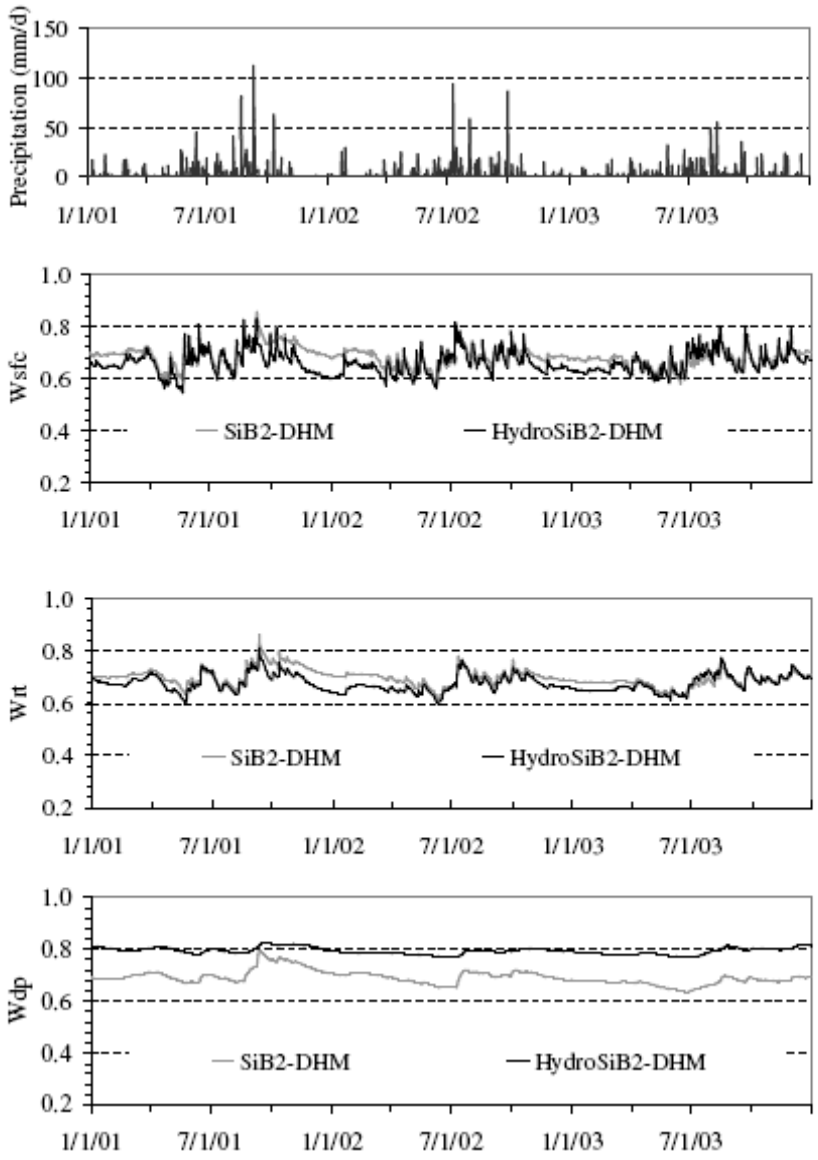

Fig. 8 Comparison of simulated soil wetness in surface layer (W_{sfc}), root zone (W_{rt}), and deep soil (W_{dp}) between SiB2-DHM and HydroSiB2-DHM from 2001 to 2003.

was determined considering both the vertical flow from the surface soil and the inverse recharges from the groundwater aquifer. It will also be affected by lateral losses in sub-layers in the root zone when their wetness is greater than the field capacity.

Figure 9 shows the difference in the simulated daily bare soil evaporation from 2001 to 2003 between the two models. SiB2-DHM generally gave higher bare soil evaporation owing to higher surface wetness. In recession periods, the increase in bare soil evaporation was near 0.1 mm/d. The difference was not negligible because the mean daily evapotranspiration for the study basin from 2001 to 2003 is less than 1.6 mm/d.

Figure 10 presents the differences in simulated daily-mean latent and sensible heat fluxes from 2001 to 2003 between the two models. Higher surface wetness simulated by the SiB2-DHM model caused an increase in latent heat flux up to 3.9 W/m^2 and a decrease in sensible heat flux up to 3.2 W/m^2, equivalent to 8.7% and 14.0% of their mean values (44.7 and 22.9 W/m^2), respectively.

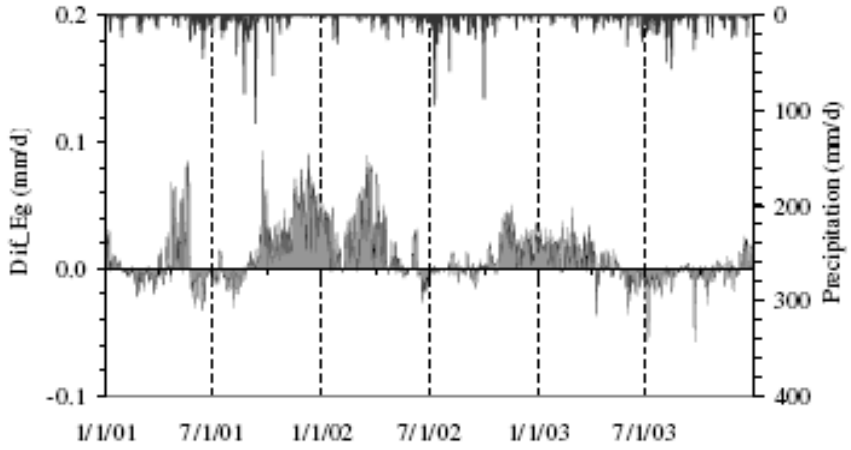

Fig. 9 Difference (SiB2-DHM minus HydroSiB2-DHM) of simulated daily bare soil evaporation from 2001 to 2003.

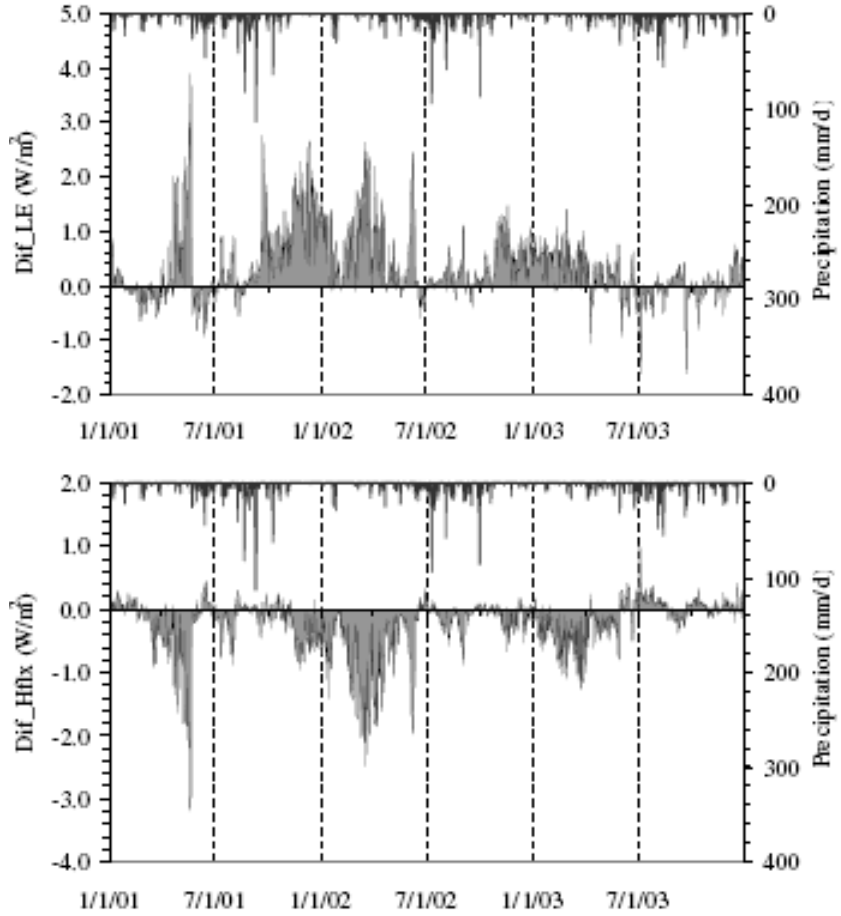

Fig. 10 Difference (SiB2-DHM minus HydroSiB2-DHM) of simulated daily mean latent (upper) and sensible (lower) heat fluxes from 2001 to 2003.

Figure 11 shows the equilibrium WTD simulated by HydroSiB2-DHM from 2001 to 2003. Although no observations were available for the validation of the WTD, the simulated WTD shows reasonable responses to precipitation events.

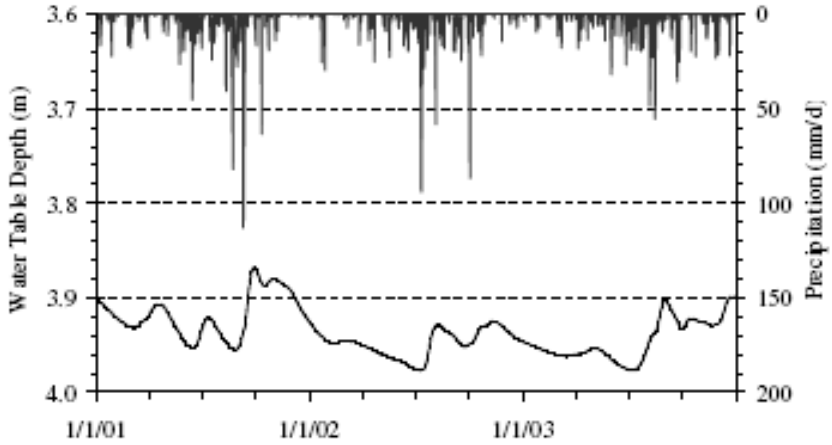

Fig. 11 Equilibrium water table depth (WTD) simulated by HydroSiB2-DHM from 2001 to 2003, where WTD takes positive in a downward direction normal to the soil surface.

It is possible for SiB2-DHM to obtain a better hydrograph by tuning soil parameters, such as using lower-conductivity soils to increase surface runoff. However, this will have a questionable impact on the model feedback. The use of lower conductivity soils in model simulation will result in a wetter surface. The simulation will then produce not only higher surface runoff, but also increased evaporation, which will make the simulation of atmospheric fluxes even worse. Another way to improve the hydrographs of SiB2-DHM is to use a smaller value for D_s. Figure 12 shows the daily hydrograph, the changes in the simulated surface soil wetness and root zone wetness, and the increase in latent heat flux simulated by SiB2-DHM with a decrease in D_s from 4 m to 2 m. However, the results show that the improvement in the daily hydrograph is at the expense of increased surface soil wetness and also an increase in latent heat flux, which will aggravate flux calculation.

CONCLUDING REMARKS

In this paper, several significant improvements of the hydrology of SiB2 have been achieved using a previous distributed hydrological model (the GBHM): (1) The SiB2 three-layer soil model is replaced by a multi-layer soil column coupled to a lumped unconfined aquifer model, which simultaneously receives the recharge from the upper soils and discharges runoff into rivers. The total thickness of the unsaturated soil changes with fluctuations of the water table. (2) Lateral flows are described in the new scheme (HydroSiB2). Overland flow is described by Manning's equation, while lateral subsurface flow and groundwater discharge are simulated using Darcy's law. (3) The soil hydraulic function in SiB2 (the Campbell/Clapp-Hornberger parameterization) is updated with the van Genuchten function, and soil vertical heterogeneity is described.

Evaluations of HydroSiB2 were performed under the spatial framework of a distributed hydrological model using available streamflow observations at different temporal frequencies. Both SiB2 and HydroSiB2 were embedded into the distributed framework of the grid-based GBHM, and SiB2-DHM and HydroSiB2-DHM were obtained. Through equilibrium simulations for a small humid river basin and using soil parameters following Yang *et al*. (2004) and vegetation parameters following Sellers *et al*. (1996b), HydroSiB2-DHM is found to perform well not only in representing the inter-annual and seasonal variations in streamflow, but also in producing reasonable daily and hourly hydrographs; while SiB2-DHM captures the characteristics of inter-annual and seasonal runoff changes but performs poorly in finer temporal-scale (daily and hourly) simulations.

Owing to the treatment of lateral flows and using a multi-layer soil model coupled with a lumped unconfined aquifer, the soil moisture budget was qualitatively improved in HydroSiB2.

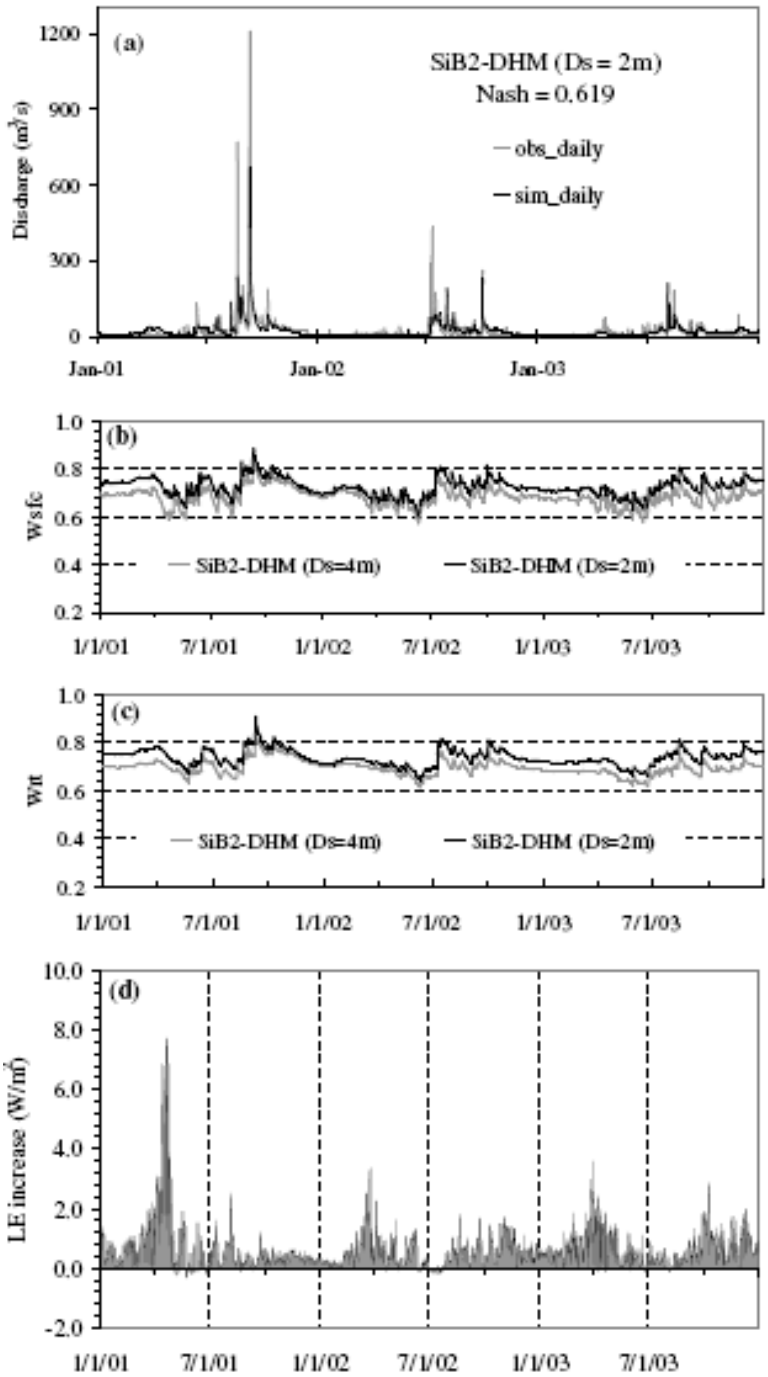

Fig. 12 Daily hydrograph (a), the changes of simulated surface soil wetness (b) and root zone wetness (c), and the increase of latent heat fluxes (d) from 2001 to 2003 simulated by SiB2-DHM with the decrease of D_s from 4 m to 2 m.

Compared to SiB2-DHM, HydroSiB2-DHM generally simulates a lower latent heat flux and a higher sensible heat flux in recession periods, which can be ascribed to the drier surface introduced by topographically driven lateral moisture redistributions.

As a hydrologically improved version of SiB2, HydroSiB2 can be coupled with mesoscale atmospheric models or general circulation models for improved water and energy flux predictions from regional to global scales.

Acknowledgements This study was funded by Core Research for Evolutional Science and Technology of the Japan Science and Technology Corporation. Parts of this work were also supported by the Ministry of Education, Culture, Sports, Science and Technology of Japan. The authors thank Dr Shinjiro Kanae and Dr Pat Jen-Feng Yeh for their helpful comments on this paper.

REFERENCES

Boone, A. Habets, F., Noilhan, J., Clark, D., Dirmeyer, P., Fox, S., Gusev, Y., Haddeland, I., Koster, R., Lohmann, D., Mahanama, S., Mitchell, K., Nasonova, O., Niu, G. Y., Pitman, A., Polcher, J., Shmakin, A. B., Tanaka, K., van den Hurk, B., Verant, S., Verseghy, D., Viterbo, P. & Yang, Z. L. (2004) The Rhone-aggregation land surface scheme intercomparison project: an overview. *J. Climate* **17**, 187–208.

Bounoua, L., Masek, J. & Tourre, Y. M. (2006) Sensitivity of surface climate to land surface parameters: a case study using the simple biosphere model SiB2. *J. Geophys. Res.* **111**, D22S09, doi:10.1029/2006JD007309.

Braun, F. J. & Schadler, G. (2005) Comparison of soil hydraulic parameterizations for mesoscale meteorological models. *J. Appl. Met.* **44**, 1116–1132.

Cabral, M. C., Garrote, L., Bras, R. L. & Entekhabi, D. (1992) A kinematic model of infiltration and runoff generation in layered and sloped soils. *Adv. Water Resour.* **15**, 311–324.

Campbell, G. S. (1974) Simple method for determining unsaturated conductivity from moisture retention data. *Soil Sci*. **117,** 311–314.

Clapp, R. B. & Hornberger, G. M. (1978) Empirical equations for some soil hydraulic properties. *Water Resour. Res*. **14**, 601–604.

Crawford, T. M. & Duchon, C. E. (1999) An improved parameterization for estimating effective atmospheric emissivity for use in calculating daytime downwelling longwave radiation. *J. Appl. Met*. **38**, 474–480.

Decharme, B. & Douville, H. (2006) Introduction of a sub-grid hydrology in the ISBA land surface model. *Climate Dynamics* **26**, 65–78.

Decharme, B., Douville, H., Boone, A., Habets, F. & Noilhan, J. (2006) Impact of an exponential profile of saturated hydraulic conductivity within the ISBA LSM: Simulations over the Rhone basin. *J. Hydromet*. **7**, 61–80.

Dickinson, R. E., Shaikh, M., Bryant, R. & Graumlich, L. (1998) Interactive canopies for a climate model. *J. Climate* **11**, 2823–2836.

Dunne, T. & Black, R. D. (1970) Partial area contributions to storm runoff in a small New-England watershed. *Water Resour. Res*. **6**, 1296–1311.

Entin, J. K., Robock, A., Vinnikov, K. Y., Zabelin, V., Liu, S., Namkhai, A. & Adyasuren, T. (1999) Evaluation of Global Soil Wetness Project soil moisture simulations. *J. Met. Soc. Japan* **77**, 183–198.

FAO (2003) Digital soil map of the world and derived soil properties, Land and Water Digital Media Series Rev. 1, CD-ROM. UN Food and Agriculture Organization, Rome, Italy.

Findell, K. L. & Eltahir, E. A. B. (2003) Atmospheric controls on soil moisture-boundary layer interactions. Part I: Framework development. *J. Hydromet*. **4**, 552–569.

Freeze, R. A. (1974) Streamflow generation. *Rev. Geophys*. **12**, 627–647.

Gao, Z., Chae, N., Kim, J., Hong, J., Choi, T. & Lee, H. (2004) Modeling of surface energy partitioning, surface temperature, and soil wetness in the Tibetan prairie using the Simple Biosphere Model 2 (SiB2). *J. Geophys. Res*. **109**, D06102. doi:10.1029/2003JD004089.

Gulden, L. E., Rosero, E., Yang, Z., Rodell, M., Jackson, C. S., Niu, G., Yeh, P. J. F. & Famiglietti, J. (2007) Improving land-surface model hydrology: Is an explicit aquifer model better than a deeper soil profile? *Geophys. Res. Lett*. **34**, L09402. doi:10.1029/2007GL029804.

Henderson-Sellers, A., Yang, Z. & Dickinson, R. E. (1993) The project for intercomparison of land surface parameterization schemes. *Bull. Am. Met. Soc.* **74**, 1335–1349.

Lohmann, D. Lettenmaier, D. P., Liang, X., Wood, E. F., Boone, A., Chang, S., Chen, F., Dai, Y. J., Desborough, C., Dickinson, R. E., Duan, Q. Y., Ek, M., Gusev, Y. M., Habets, F., Irannejad, P., Koster, R., Mitchell, K. E., Nasonova, O. N., Noilhan, J., Schaake, J., Schlosser, A., Shao, Y. P., Shmakin, A. B., Verseghy, D., Warrach, K., Wetzel, P., Xue, Y. K., Yang, Z. L. & Zeng, Q. C. (1998) The Project for Intercomparison of Land-surface Parameterization Schemes (PILPS) Phase 2(c) Red–Arkansas River basin experiment: 3. Spatial and temporal analysis of water fluxes. *Global Planet. Change* **19**, 161–179.

Manabe, S. (1969) Climate and ocean circulation. I. Atmospheric circulation and circulation and hydrology of Earth's surface. *Mon. Weather Rev*. **97**, 739–774.

Maxwell, R. M., Chow, F. K. & Kollet, S. J. (2007) The groundwater–land-surface–atmosphere connection: soil moisture effects on the atmospheric boundary layer in fully-coupled simulations. *Adv. Water Resour*. **30**, 2447–2466.

Myneni, R. B., Nemani, R. R. & Running, S. W. (1997) Estimation of global leaf area index and absorbed PAR using radiative transfer models. *IEEE. Trans. Geosci. Remote Sens.* **35,** 1380–1393.

Nash, J. E. & Sutcliffe, J. V. (1970) River flow forecasting through conceptual models, Part I: A discussion of principles. *J. Hydrol*. **10**(3), 282–290.

Niu, G., Yang, Z., Dickinson, R. E., Gulden, L. E. & Su, H. (2007) Development of a simple groundwater model for use in climate models and evaluation with Gravity Recovery and Climate Experiment data. *J. Geophys. Res*. **112**, D07103. doi:10.1029/2006JD007522.

Pfafstetter, O. (1989) Classification of hydrographic basins: coding methodology. Unpublished manuscript, 18 August 1989 Departamento Nacional de Obras de Saneamento, Rio de Janeiro, Brazil.

Pielke, R. A. (2001) Influence of the spatial distribution of vegetation and soils on the prediction of cumulus convective rainfall.

Rev. Geophys. **39**, 151–177.

Randall, D. A., Dazlich, D. A., Zhang, C., Denning, A. S., Sellers, P. J., Tucker, C. J., Bounoua, L., Los, S. O., Justice, C. O. & Fung, I. (1996) A revised land surface parameterization (SiB2) for GCMs. 3. The greening of the Colorado State University general circulation model. *J. Climate* **9**, 738–763.

Rawls, W. J. & Brakensiek, D. L. (1982) Estimating soil water retention from soil properties. *J. Irrig. Drain. Div. ASCE* **108**, 166–171.

Robinson, J. S. & Sivapalan, M. (1996) Instantaneous response functions of overland flow and subsurface stormflow for catchment models. *Hydrol. Processes* **10**, 845–862.

Sellers, P. J., Mintz, Y., Sud, Y. C. & Dalcher, A. (1986) A simple biosphere model (SiB) for use within general circulation models. *J. Atmos. Sci*. **43**, 505–531.

Sellers, P. J., Los, S. O., Tucker, C. J., Justice, C. O., Dazlich, D. A., Collatz, G. J. & Randall, D. A. (1996a) A revised land surface parameterization (SiB2) for atmospheric GCMs. 2. The generation of global fields of terrestrial biophysical parameters from satellite data. *J. Climate* **9**, 706–737.

Sellers, P. J., Randall, D. A., Collatz, G. J., Berry, J. A., Field, C. B., Dazlich, D. A., Zhang, C., Collelo, G. D. & Bounoua, L. (1996b) A revised land surface parameterization (SiB2) for atmospheric GCMs. 1. Model formulation. *J. Climate* **9**, 676–705.

Soulis, E. D., Snelgrove, K., Kouwen, N., Seglenieks, F. & Verseghy, D. L. (2000) Towards closing the vertical water balance in Canadian atmospheric models: coupling of the land surface scheme CLASS with the distributed hydrological model WATFLOOD. *Atmos. Ocean* **38**(1), 251–269.

Tang, Q., Oki, T. & Kanae, S. (2006) A distributed biosphere hydrological model (DBHM) for large river basin. *Ann. J. Hydraul. Engng Japan Soc. Civil Engrs* **50**, 37–42.

Tang, Q., Oki, T., Kanae, S. & Hu, H. (2008) Hydrological cycles change in the Yellow River basin during the last half of the 20th century. *J. Climate* **21**(8), 1790–1806. doi:10.1175/2007JCLI1854.1.

van Genuchten, M. T. (1980) A closed form equation for predicting the hydraulic conductivity of unsaturated soils. *Soil Sci. Soc. Am. J*. **44**, 892–898.

Verdin, K. L. & Verdin, J. P. (1999) A topological system for delineation and codification of the Earth's river basins. *J. Hydrol.* **218**, 1–12.

Wang, L., Wang, Z., Yin, H., Yang, D. & He, S. (2006) A distributed hydrological model–GBHM and its application in a middle–scale catchment (in Chinese). *J. Glaciol. Geocryol.* **28**(2), 256–261.

Yang, D., Herath, S. & Musiake, K. (2000) Comparison of different distributed hydrological models for characterization of catchment spatial variability. *Hydrol. Processes* **14**, 403–416.

Yang, K., Huang, G. & Tamai, N. (2001) A hybrid model for estimating global solar radiation. *Solar Energy* **70**, 13–22.

Yang, D., Herath, S. & Musiake, K. (2002) A hillslope-based hydrological model using catchment area and width functions. *Hydrol. Sci. J*. **47**(1)**,** 49–65.

Yang, D., Koike, T. & Tanizawa, H. (2004) Application of a distributed hydrological model and weather radar observations for flood management in the upper Tone River of Japan. *Hydrol. Processes* **18**, 3119–3132.

Yang, K., Koike, T. & Ye, B. (2006) Improving estimation of hourly, daily, and monthly solar radiation by importing global data sets. *Agric. For. Met*. **137**, 43–55.

Yeh, P. J. F. & Eltahir, E. A. B. (2005) Representation of water table dynamics in a land surface scheme. Part I: Model development. *J. Climate* **18**, 1861–1880.

Received 26 September 2008; accepted 3 May 2009